

ISSN No. 2454-6194 | DOI: 10.51584/IJRIAS | Volume X Issue IX September 2025

New Boron Deposition Model Based on Thin Oxide Film in Process of High Frequency Transistor

NamChol Yu¹*, IIRyong Bong², ChenNam Kim³, SongChol Yang⁴

¹Kim Chaek University of Technology, Pyongyang, Democratic People's Republic of Korea

²Sariwon College of Technology, North HuangHae, Democratic People's Republic of Korea

³University of Science, Pyongyang, Democratic People's Republic of Korea

⁴Pyongsong University of Education, South Pyongan, Democratic People's Republic of Korea

*Corresponding Author

DOI: https://dx.doi.org/10.51584/IJRIAS.2025.100900097

Received: 16 August 2025; Accepted: 23 August 2025; Published: 25 October 2025

ABSTRACT

This paper reports new deposition model of boron impurity considered formation of oxide film during deposition process. Finally, we have considered the impurity concentration change in silicon surface and found that diffusion coefficient in the thin oxide film increases more 100 times than the thick oxide film. The result contributes to get the accurate simulation value. This new boron deposition model will apply to find the formation condition of base layer in fabrication process of high-frequency transistor.

Keyword: Boron impurity; Deposition model; Concentration distribution; Diffusion coefficient.

INTRODUCTION

It is able to simulate the deposition process through oxide film by SILVACO TCAD (semiconductor process simulation tools), but the simulation results did not give the accurate values.

The impurity deposition is progressing after formation of the thin oxide film [1-3].

Recently, many research results about the boron deposition process reports [4-18], but the simulation results about sheet resistance, junction depth and impurity quantity as control factor of the fabrication process of semiconductor device have not correctly calculated in deposition process simulation of boron impurity.

Therefore, we proposed the deposition model of boron impurity and the diffusion factors of oxide film using to calculate have changed for the accurate simulation.

New Model

At silicon surface, always exists the natural oxide film or oxide film formed during boron deposition process, and boron impurity diffuses through the oxide film into silicon



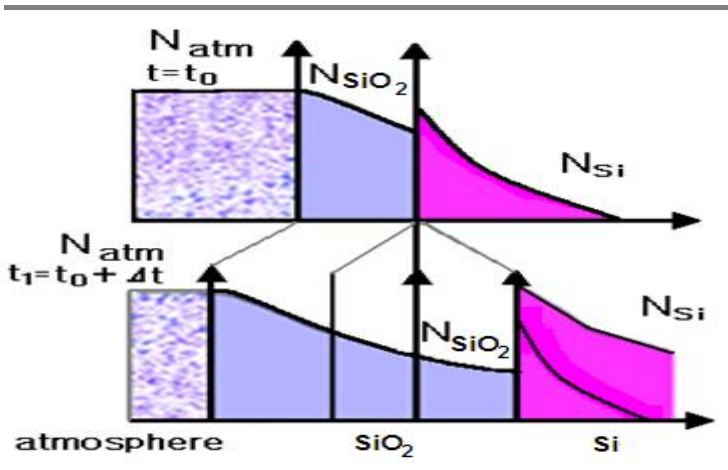


Fig.1 Impurity flow in deposition process of boron impurity

In silicon surface, boron impurity concentration is not fixed, it increase gradually and oxide film thickness is increased. Therefore, we have shown intuitionally the impurity concentration in atmosphere, oxide film and silicon as Fig.1. Where N_{atm} is impurity concentration in atmosphere, N_{SiO2} is impurity concentration in oxide film, N_{si} is impurity concentration in silicon. The corresponding mathematical model can write as follows. If thickness is very thin, impurity diffusion in oxide film can approximate linearly as follows;

$$J_{p} = k_{INC} D_{SiO_{2}} \frac{N_{SiO_{2}}}{d_{SiO_{2}}}$$
 (1)

Where k_{INC}- increase coefficient of diffusion coefficient in oxide film

D_{SiO2}-diffusion coefficient in oxide film

N_{SiO2}-impurity concentration in oxide film surface

dsio2- oxide film thickness

We suppose that the impurity flow diffused through the Si-SiO₂ interface is equal with impurity flow in oxide film.

Then, at the Si-SiO₂ interface, the impurity concentration relationship in oxide film and silicon determined by segregation coefficient as follows equation (2).

$$mN_{SiO_2} = N_{Si}, \quad x = 0, t \ge 0$$
 (2)

Here m is function of temperature as a segregation coefficient.

Here, we used the condition that the ratio of impurity concentration in oxide film and silicon is constant under defined temperature. In silicon bulk, the peak's diffusion law is applied.

$$\frac{\partial N_{Si}}{\partial t} = \frac{\partial}{\partial X} \left(\frac{\partial (D_{si} \cdot N_{si})}{\partial X} \right), \quad X \in \Omega$$
(3)

Here N_{Si}- boron impurity concentration in silicon

D_{Si}- diffusion coefficient of the boron impurity changing due to concentration in silicon

t - deposition time

Ω - internal region of silicon

ISSN No. 2454-6194 | DOI: 10.51584/IJRIAS | Volume X Issue IX September 2025



Then, if the impurity concentration at relatively far region from the silicon-oxide film interface is not change with distance, it can write as follows equation (4)

$$\frac{\partial N_{si}}{\partial X} = 0, \quad X = \infty$$
 (4)

Starting condition (impurity concentration before the deposition) is as follows

$$N_{si}(X,0) = N_{si}(X), \quad t = 0, \quad X = (0 \sim \infty)$$
 (5)

Finally, we can find out the concentration distribution of boron impurity in silicon by these equations (1)-(5). We have used that vacancy diffusion mechanism is fundamental in boron diffusion. The boron diffusion coefficient in silicon and oxide film did used from literature [2, 5].

Simulation results by SILVACO TCAD

The impurity concentration of the starting wafer is $4\times10^{12} \text{cm}^{-3}$, major facets is {111} plane and substrate is n-type silicon. As shown in Fig.2, since surface impurity concentration is about 10^{14}cm^{-3} , junction depth is $0.077 \mu \text{m}$ and sheet resistance is $1.3\times10^{9} \Omega/\Box$, the difference between simulation result and actually measurement value is very large. Because diffusion coefficient used in simulating is incorrect.

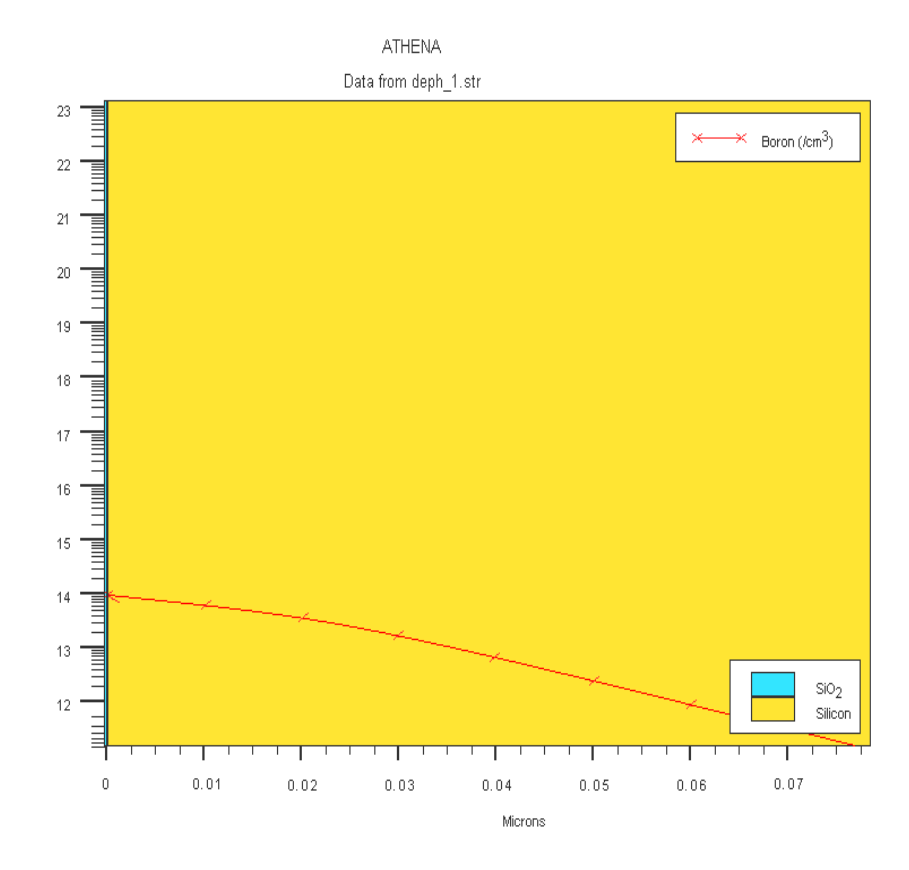


Fig.2 Deposition simulation (concentration distribution) result by SILVACO TCAD(950°C)

The diffusion coefficient in oxide film explained as follows:

$$D = D_0 \exp(-E/KT) \tag{6}$$

Where D is diffusion coefficient(cm²/s), D_0 is 7.23×10^{-6} as the coefficient of exponent term, E is 3.5eV as the activation-energy. The difference between simulation result of boron deposition process with default value and the actually measurement values is very large. So we have assumed that k_{inc} is 100, impurity concentration is 3×10^{21} cm⁻³ in gas phase-SiO₂ interface. The simulation result at 950°C shows in Fig.3.



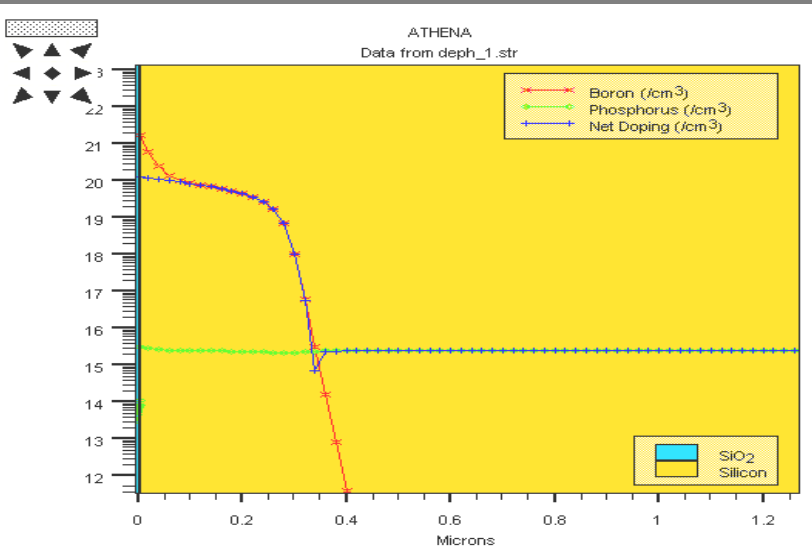


Fig.3 Impurity concentration distribution of boron deposition by simulation

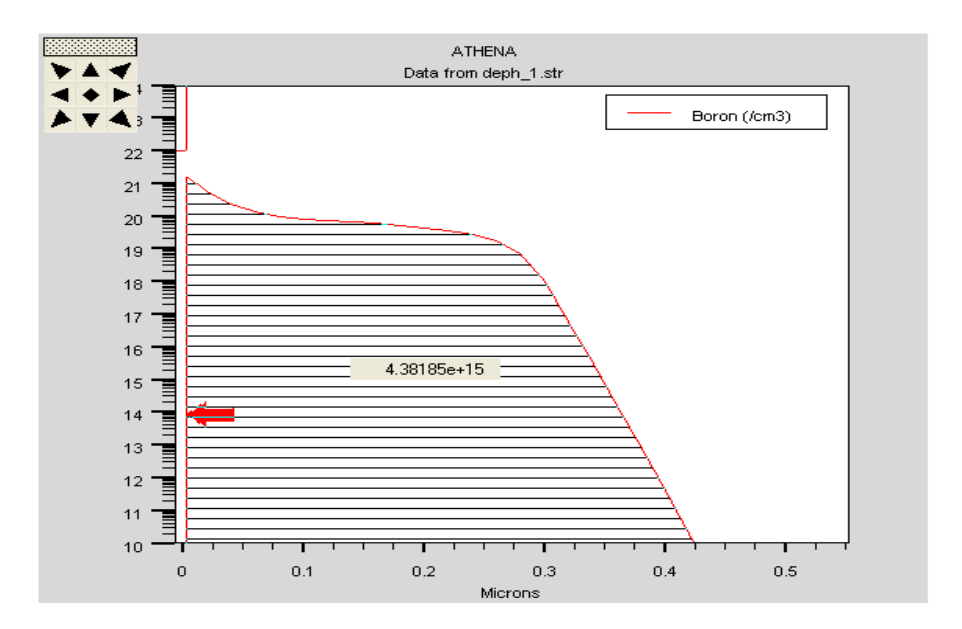


Fig.4 Calculation result of the impurity mass after boron deposition

The impurity mass was obtained by integral of concentration graph, as shown in Fig.4. The simulation result about deposition process at difference temperature gives in table 1.

Table 1 The calculation result of sheet resistance and the impurity mass due to deposition temperature

Deposition temperature (°C)	$\begin{array}{cc} \text{Sheet} & \text{resistance} \\ (\Omega/\Box) & \end{array}$	Impurity mass(cm ⁻²)	Activity impurity mass (cm ⁻²)	Junction depth (µm)
850	317.45	1.22×10 ¹⁵	3.89×10 ¹⁴	0.15
900	113.56	2.63×10 ¹⁵	1.05×10 ¹⁵	0.27
950	43.88	6.21×10 ¹⁵	2.66×10 ¹⁵	0.49
970	30.50	8.77×10^{15}	3.82×10 ¹⁵	0.62
975	27.93	9.65×10 ¹⁵	4.17×10 ¹⁵	0.66

S S

ISSN No. 2454-6194 | DOI: 10.51584/IJRIAS | Volume X Issue IX September 2025

980	25.54	1.10×10 ¹⁶	5.09×10 ¹⁵	0.70
990	21.42	1.25×10 ¹⁶	5.42×10 ¹⁵	0.78
1 000	18.06	1.48×10 ¹⁶	6.42×10 ¹⁵	0.88
1 020	12.86	2.23×10 ¹⁶	1.04×10 ¹⁶	1.10
1 030	10.89	2.472×10 ¹⁶	1.06×10 ¹⁶	1.23
1 050	7.89	3.55×10 ¹⁶	1.59×10 ¹⁶	1.53
1 060	6.72	4.04×10 ¹⁶	1.71×10 ¹⁶	1.71
1 070	5.75	4.70×10 ¹⁶	1.99×10 ¹⁶	1.91

Experimental verification of boron deposition process

We compared the exactly experiment results and the simulation at the difference temperature for accuracy of simulation results. Comparison item is sheet resistance and junction depth. Finally, measurement result was a very approximation to the simulation result.

Table 2 Experimental verification result of sheet resistance and junction depth due to the deposition temperature

Deposition temperature(°C)	Simulation result		Measurement result	
	Sheet resistance(Ω/\Box)	Junction depth(μm)	Sheet resistance(Ω/\Box)	Junction depth(μm)
850	317.45	0.15	329	0.11
900	113.56	0.27	110	0.3
950	43.88	0.49	45.3	0.45
970	30.50	0.62	32	0.59
975	27.93	0.66	27.1	0,64
980	25.54	0.70	23.5	0.69
1 000	18.06	0.88	18.9	0.91
1 050	7.89	1.53	7.76	1.46
1 070	5.75	1.91	5.70	1.89

CONCLUSION

Firstly, the new boron deposition model considered on oxide film is proper within deposition temperature range and it gives more right simulation result about sheet resistance and junction depth. Secondly, in deposition process simulation of boron impurity, when the impurity concentration is 3×10^{21} cm⁻³ and $k_{\rm INC}$ is 100, simulation result is equal with measurement result. Therefore, it shows that diffusion coefficient in the thin oxide film increases more 100 times than in the thick oxide film. This new boron deposition model will

ISSN No. 2454-6194 | DOI: 10.51584/IJRIAS | Volume X Issue IX September 2025



apply to find the formation condition of base layer in fabrication process of high-frequency transistor.

REFERENCES

- 1. Richard B. Fair, Unified Model of Boron Diffusion in thin Gate Oxide: Effects of F, H₂, N, Oxide film and Injected Si Interstitials, IEEE IEDM' 95 (85-88), 1995. https://doi.org/10.1109/IEDM.1995.497188
- Shiro Horiuchi and Jiro Yamaguchi, Diffusion of Boron in Silicon through oxide layer, Journal of APPLIED PHYSICS, vol.1, No.6, 50-67, 1966
- 3. M.Ghembaza, et al, Effects of Thickness and Chemical Quality of SiO₂ barrier on POCl₃ Diffusion of Emitter. Energy Procedia 733-740, during formation Vol 2012, https://doi.org/10.1016/j.egypro.2012.05.089
- 4. Roland Yingjie Tay, Hongling Li, Hong Wang, et.al, Advanced nano boron nitride architectures: Synthesis, properties and emerging applications, Nano Today, Vol. 53. https://doi.org/10.1016/j.nantod.2023.102011.
- 5. E. Brezza, F. Deprat, C. de Buttet, A. Gauthier, et.al, Optimized emitter-base interface cleaning for advanced Heterojunction Bipolar Transistors, Solid-State Electronics, Vol. 204, 2023, 108654, https://doi.org/10.1016/j.sse.2023.108654.
- 6. Grazia Lo Sciuto, Salvatore Coco, Rafi Shikler, Antonello Tamburrino, Pentacene organic thin-film transistor based on Archimedean interdigitated spiral pattern, Microelectronic Engineering, Vol. 247, 2021, 111590, https://doi.org/10.1016/j.mee.2021.111590.
- 7. João P. Braga, Cleber A. Amorim, Guilherme R. De Lima, Giovani Gozzi, Lucas Fugikawa-Santos, The role of intrinsic trap states in the semiconductor/insulating interface on the electrical performance of spray-coated thin-film transistors, Materials Science in Semiconductor Processing, Vol. 151, 2022, 106984, https://doi.org/10.1016/j.mssp.2022.106984.
- 8. Ashok Srivastava, Md S. Fahad, Vertical MoS₂/hBN/MoS₂ interlayer tunneling field effect transistor, Solid-State Electronics, Vol. 126, 2016, 96-103, https://doi.org/10.1016/j.sse.2016.09.008.
- 9. Sai Wang, Guojun Huang, Han Luo, Wei Li, Mengzhen Zhu, Xia Chen, Chaowei Mi, Improving the composition and multifunctional properties of amorphous boron nitride films prepared by postannealing assisted femtosecond pulsed laser deposition method, Ceramics International, Vol. 49, 2023, 29887-29896, https://doi.org/10.1016/j.ceramint.2023.06.246.
- 10. Aasif Mohammad Bhat, Ritu Poonia, Arathy Varghese, Nawaz Shafi, C. Periasamy, AlGaN/GaN high electron mobility transistor for various sensing applications: A review, Micro and Nanostructures, Vol. 176, 2023, 207528, https://doi.org/10.1016/j.micrna.2023.207528.
- 11. Joseph Casamento, John Hayden, Susan Trolier-McKinstry, et. al, Chapter Five Toward new ferroelectric nitride materials and devices: Aluminum boron nitride and aluminum scandium nitride ferroelectric high electron mobility transistors (FerroHEMTs), Editor(s): John Heron, Zetian Mi, Semiconductors and Semimetals, Elsevier, Vol. 114, 2023, https://doi.org/10.1016/bs.semsem.2023.09.016.
- 12. Michał Rycewicz, Adrian Nosek, Dong Hoon Shin, et. al, The effect of boron concentration on the electrical, morphological and optical properties of boron-doped nanocrystalline diamond sheets: Tuning the diamond-on-graphene vertical junction, Diamond and Related Materials, Vol. 128, 2022, 109225, https://doi.org/10.1016/j.diamond.2022.109225.
- 13. Yajuan Zhao, Zhaohui Zhang, Jianfeng Huang, et. al, Salt-promoted growth of monolayer tungsten disulfide on hexagonal boron nitride using all chemical vapor deposition approach, Applied Surface Science, Vol. 605, 2022, 154812, https://doi.org/10.1016/j.apsusc.2022.154812.
- 14. Gaokai Wang, Jingren Chen, Junhua Meng, Zhigang Yin, Ji Jiang, Yan Tian, Jingzhen Li, Jinliang Wu, Peng Jin, Xingwang Zhang, Direct growth of hexagonal boron nitride films on dielectric sapphire substrates by pulsed laser deposition for optoelectronic applications, Fundamental Research, Vol. 1, 2021, 677-683, https://doi.org/10.1016/j.fmre.2021.09.014.
- 15. Tiago Davi Curi Busarello, Marcelo Godoy Simões, José Antenor Pomilio, Chapter 2 Semiconductor Diodes and Transistors, Editor(s): Muhammad H. Rashid, Power Electronics Handbook (Fifth Edition), Butterworth-Heinemann, 2024, Pages 17-52, https://doi.org/10.1016/B978-0-323-99216-9.00027-5.
- 16. Xiaoyue Wang, Chi Liu, Yuning Wei, Shun Feng, Dongming Sun, Huiming Cheng, Three-dimensional transistors and integration based on low-dimensional materials for the post-Moore's law era, Materials





Today, Vol. 63, 2023, 170-187, https://doi.org/10.1016/j.mattod.2022.11.023.

- 17. Antonio J. Olivares, A. Zamchiy, V.S. Nguyen, P. Roca i Cabarrocas, Boron activation in silicon thin films grown by PECVD under epitaxial and microcrystalline conditions, Applied Surface Science Advances, Vol. 18, 2023, 100508, https://doi.org/10.1016/j.apsadv.2023.100508.
- 18. N. Lambert, A. Taylor, P. Hubík, J. Bulíř, J. More-Chevalier, H. Karaca, C. Fleury, J. Voves, Z. Šobáň, D. Pogany, V. Mortet, Modeling current transport in boron-doped diamond at high electric fields including self-heating effect, Diamond and Related Materials, Vol. 109, 2020, 108003, https://doi.org/10.1016/j.diamond.2020.108003.

Page 994